geoconvention
Calgary • Canada • May 13-17 2019

Effect of deconvolution operations on the elastic FWI of a walkaway VSP dataset

Raul Cova[1], Kris Innanen[1] and Marianne Rauch-Davies[2]
[1] CREWES-University of Calgary, [2] Devon Energy

Summary

We perform an elastic FWI using land VSP data acquired in a walkaway configuration. The dataset was pre-processed with two different deconvolution applications. Originally, a deterministic deconvolution using the recorded downgoing wavefield was applied to remove the source signature. Even though this process partially accounts for changes in the wavelet with depth, a single operator is used for all the events recorded on a given trace. For this reason, we also applied a Gabor deconvolution to more completely account for non-stationarity in the source signature. The FWI performed on the data deconvolved with the deterministic operators converged toward a solution that was closer to the sonic logs available in the well. Despite providing a wider frequency spectrum, the FWI using the Gabor deconvolved data did not converge toward an optimal solution. A closer examination of the input data revealed that in addition to removing some of the multiples, the deterministic deconvolution resurfaced some downgoing S-wave events that were not evident before. This provides important information for the inversion of S-wave velocities. In summary, providing data with less complexity and enhancing critical events resulted in a more robust initialization of the inversion problem.

Introduction

Full waveform inversion (FWI) can be considered a well-established method for computing high resolution earth models particularly in marine data processing. Successful results can be found in the literature that illustrate the potential of FWI in this environment (Ratcliffe et al., 2011; Operto et al., 2015; Routh et al., 2017). On land data, this goal is significantly more difficult. The reasons include, but are not limited to, very complex near-surface effects, unknown source and receiver signature, strong anelasticity and poor signal-to-noise ratio particularly for the frequencies in the low end of the spectrum. These low frequencies are usually never recorded and have to be estimated.

Podgornova et al. (2014) and Pan et al. (2018) report successful results in performing elastic FWI over land VSP datasets. On these type of data, some of the challenges of surface seismic data, like near-surface effects and signal-to-noise ratio are less problematic. Here, we focus on the pre-processing needed for the FWI to provide accurate results using a walkaway VSP dataset. The dataset we use presents very large and frequent velocity contrasts that result in very energetic short-wavelength multiples, that challenge the initialization of the inversion.

Deconvolution Tests

Two deconvolution algorithms were tested on the data. First, we tried a conventional deterministic deconvolution using the downgoing wavefield. In this type of deconvolution the frequency spectrum of the downgoing wavefield is computed and its inverse is used to construct the deconvolution operator. A window of 600 ms around the first arrivals was used for the computation

of the spectra and a pre-whitening factor of 1% was added to stabilize the inversion of the deconvolution operators.

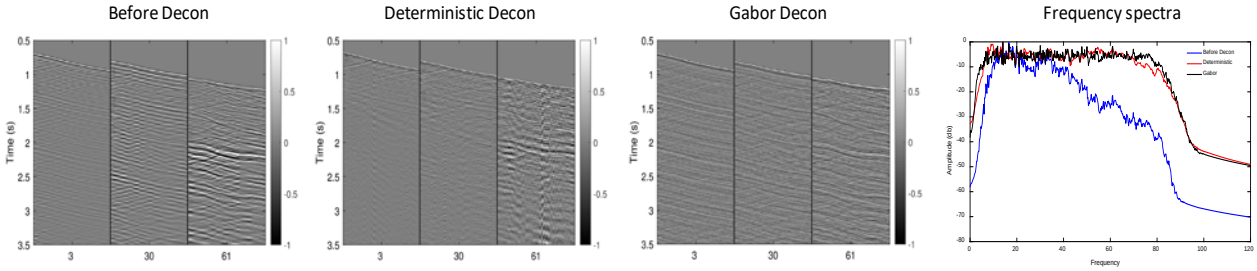

Figure 1. Data before and after deterministic and Gabor deconvolutions and their frequency spectra.

A subset of the vertical component data, before and after deconvolution, are displayed on Figure 1. There we can see how the character of the events has been sharpened and the frequency spectra have been equalized for the band between 4 Hz and 80 Hz. This can be confirmed in the average frequency spectra presented in Figure 1. Of particular interest for FWI is the improvement of the frequency content on the lower end of the spectrum. In this case, after deconvolution we have gained about 20 db on the frequencies between 4 Hz and 10 Hz.

In order to compensate for anelastic effects we also considered applying a Gabor deconvolution (Margrave and Lamoureux, 2001) to the data. With this type of deconvolution we aim to remove time-dependent source wavelet variations in a more complete fashion. The deconvolution was performed using windows of 0.2 s in increments of 0.01 s and temporal and frequency smoothers of 0.4 s and 4 Hz, respectively.

The vertical component after Gabor deconvolution are also shown in Figure 1. Similar to the deterministic deconvolution, the Gabor-deconvolved data resulted in in a wider and more equalized frequency spectrum. Moreover, the events after Gabor deconvolution display better coherency and the amount of noise introduced by this deconvolution is much lower. The flat character of the frequency spectrum between 4 Hz and 80 Hz is very clear in Figure 1. Significant gains in the low end of the spectrum are also evident with this deconvolution method.

Full Waveform Inversion

We used a time domain elastic FWI algorithm based on spectral elements modelling (Komatitsch and Tromp, 1999). We defined a mesh with an element size of 25 m and 5 Gauss-Lobatto-Legendre (GLL) points per element. This resulted in a minimum distance between points of 4.31 m. The modelling time step was set at 3.25×10^{-4} s to satisfy the CFL stability condition. The initial velocity and density models were computed by smoothing the available well log data using a Gaussian smoother with a half-length of 100 m.

The inversion was carried out in three depth windows: 250 - 1000 m, 750 - 2250 m and 2000 - 3500 m. At each depth window the inversion was performed using a multi-scale approach with four expanding frequency bands from [4 Hz, 8 Hz] to [4 Hz, 12 Hz], [4 Hz, 16 Hz] and [4 Hz, 20 Hz]. Eight source locations were used in the inversion ranging between 113 m and 1812.5 m offset from the well.

Figure 2 shows the near-offset data for the first scale and first depth window. The effects of the pre-processing are very clear in this example. On the data deconvolved with the deterministic operators it is possible to identify a downgoing S-wave arrival that was not evident in the data before deconvolution and is not observable in the Gabor-deconvolved data. The deterministic deconvolution, by trying to deconvolve the downgoing wavelet, collapsed most of the downgoing P-wave energy around the direct arrivals revealing the downgoing S-wave energy present in the data.

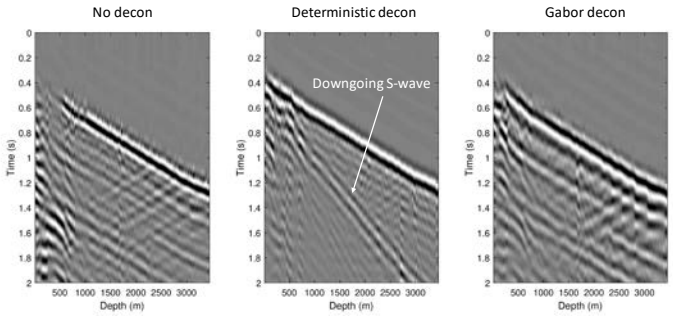

Figure 2. Data filtered between [4-8 Hz].

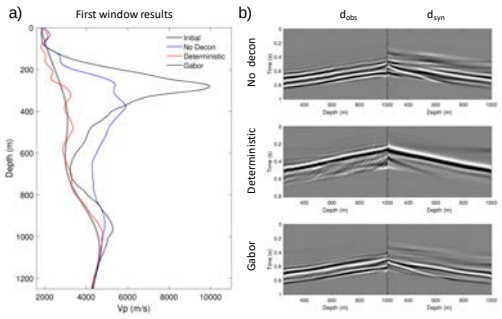

Figure 3. (a) Inverted Vp models using the downgoing wavefields. (b) Downgoing observed and modelled data after FWI.

To test the performance of the inversion on both scenarios, we first inverted the downgoing wavefield of the near-offset source with both types of deconvolution. The downgoing wavefield was separated from the full wavefield on-the-fly by using an FK filter, suppressing all the negative wavenumbers. Only the data within a 500 ms window centered around the first arrivals were used for the inversion, the rest of the data were muted. The inverted Vp values for this test using the first depth window are shown in Figure 3a. There, we can observe that the inversion performed with the Gabor deconvolved data is diverging significantly from the initial Vp model. Using data without any deconvolution also resulted in a divergent solution. Only the data deconvolved with deterministic operators show a stable solution, providing reasonable model updates around the initial Vp model. These observations can be confirmed on the data space (Figure 3b) where only the data modelled after the inversion with the deterministic deconvolution closely resembles the observed data.

The previous results can be explained by the presence of long and short period interbed multiples in the data. In particular, the presence of fine layering with large velocity contrasts that results in very short-period internal multiples, introduces a coda in the downgoing wavefield that is very difficult to explain with an initial smooth velocity model.

Based on the previous results we chose to proceed with the inversion using only the data with deterministic deconvolution. We inverted for Vp and Vs, keeping the density model fixed. The results at the location of the well are shown in Figure 4. Overall, the inverted Vp values follow very closely the expected values according to the well log. However, the inversion underestimated the actual Vp values in the section around 1500 m depth. The results for Vs also show a good agreement in the shallow part of the section. However, for depths under 2000 m the results are mixed. We would expect these results to improve by including farther source locations with more energetic S-wave arrivals in the inversion.

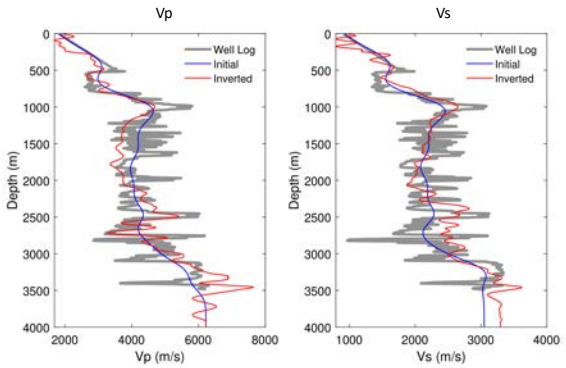

Figure 4. FWI results at the well location.

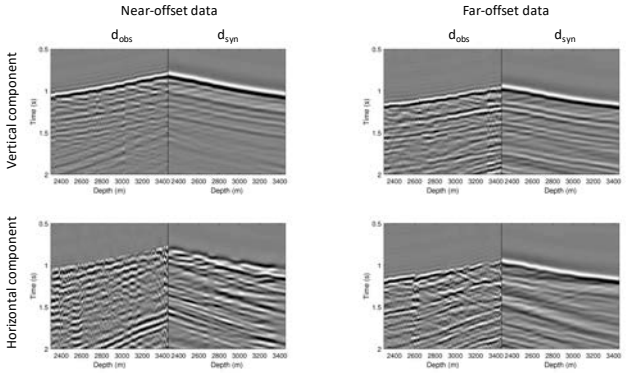

Figure 5. Observed and modelled data at the near and far offset locations, after FWI.

Figure 5 compares the observed data and the data modelled with the inverted model for a near- and far-offset locations. There we can see a good agreement between the modelled and observed downgoing wavefields, particularly for the vertical component data at both offsets. Even some of the downgoing multiples that were attenuated in the data used for the inversion, have been reproduced. On the horizontal components the results are mixed. For the near-offset data there is very little coherent energy above 1.5 s. There is a large-amplitude S-wave event around 1.75 s that is partially matched on the synthetic data. However, their frequency content is slightly different. On the observed far-offset data S-wave energy displays better coherency. There, we can observe a better agreement among the downgoing events on both datasets.

Conclusions

The non-linearity of the FWI problem can lead to very different solutions given small perturbations, not only in the model space but also in the data domain. We inverted one dataset pre-processed with two different deconvolution methods that were trying to account for the missing physics (anelasticity) in our FWI algorithm. The results obtained with a simple deterministic deconvolution were superior than the ones obtained with a Gabor deconvolution. We argue that by collapsing and attenuating some of the multiples present in the data, the deterministic deconvolution provided an easier-to-model dataset given a smooth initial velocity model. Moreover, by attenuating the multiples the deterministic deconvolution was able to reveal some downgoing S-wave events that were not evident before. The Gabor deconvolution certainly provided a wider and more stable amplitude spectrum, but it left the energy resulting from multiple events untouched, resulting in a more complex dataset. In this case, a more complex initial subsurface model might be needed for the inversion to converge toward a reasonable model.

Acknowledgements

The authors thank the sponsors of CREWES in particular to Devon Energy for facilitating the data used in this study. This work was funded by CREWES industrial sponsors, CFREF (Canada First Research Excellence Fund) and NSERC (Natural Science and Engineering Research Council of Canada) through the grant CRDPJ 461179-13. We are also grateful to Compute Canada for providing the computational resources used in this study.

References

Komatitsch, D., and Tromp, J., 1999, Introduction to the spectral-element method for 3-D seismic wave propagation: Geophysical Journal International, 139, No. 3, 806–822.

Margrave, G., and Lamoureux, M., 2001, Gabor deconvolution: CREWES Research Report, 13, 241–276.

Operto, S., Miniussi, A., Brossier, R., Combe, L., Metivier, L., Monteiller, V., Ribodetti, A., and Virieux, J., 2015, Efficient 3-d frequency-domain mono-parameter full-waveform inversion of ocean-bottom cable data: application to valhall in the visco-acoustic vertical transverse isotropic approximation: Geophysical Journal International, 202, No. 2, 1362–1391.

Pan, W., Innanen, K. A., and Geng, Y., 2018, Elastic full-waveform inversion and parametrization analysis applied to walk-away vertical seismic profile data for unconventional (heavy oil) reservoir characterization: Geophysical Journal International, 213, No. 3, 1934–1968.

Podgornova, O., Leaney, S., Charara, M., and Lunen, E. V., 2014, Elastic full waveform inversion for land walkaway VSP data: CSEG Geoconvention 2014 Expanded abstracts.

Ratcliffe, A.,Win, C., Vinje, V., Conroy, G.,Warner, M., Umpleby, A., Stekl, I., Nangoo, T., and Bertrand, A., 2011, Full waveform inversion: A north sea obc case study: SEG Technical Program Expanded Abstracts 2011, 2384–2388.

Routh, P., Neelamani, R., Lu, R., Lazaratos, S., Braaksma, H., Hughes, S., Saltzer, R., Stewart, J., Naidu, K., Averill, H., Gottumukkula, V., Homonko, P., Reilly, J., and Leslie, D., 2017, Impact of high-resolution FWI in the western black sea: Revealing overburden and reservoir complexity: The Leading Edge, 36, No. 1, 60–66.